Journal of Biomechanics 141 (2022) 111169

Contents lists available at ScienceDirect

Journal of Biomechanics

journal homepage: www.elsevier.com/locate/jbiomech

Recovery from sagittal-plane whole body angular momentum perturbations during walking

M. van Mierlo [a,*], J.I. Ambrosius [a], M. Vlutters [a], E.H.F. van Asseldonk [a], H. van der Kooij [a,b]

[a] Department of Biomechanical Engineering, University of Twente, Enschede, The Netherlands
[b] Department of Biomechanical Engineering, Delft University of Technology, Delft, The Netherlands

ARTICLE INFO

Keywords:
Human balance
Gait
Whole body angular momentum
Centre of pressure modulation
Ground reaction force vector

ABSTRACT

Healthy individuals highly regulate their whole body angular momentum (WBAM) during walking. Since WBAM regulation is essential in maintaining balance, a better understanding is required on how healthy individuals recover from WBAM perturbations. We therefore studied how healthy individuals recover WBAM in the sagittal plane. WBAM can be regulated by adjusting the moment arm of the ground reaction force (GRF) vector with respect to the whole-body centre of mass (CoM). In principle this can be done by centre of pressure (CoP) modulation and/or adjustments of the GRF direction. Two simultaneous perturbations of the same magnitude were applied in opposite direction to the pelvis and upper body (0.34 m apart) to perturb WBAM but not the whole body linear momentum (WBLM), while participants walked on a treadmill. The perturbations were given at toe off right, had a magnitude of 4, 8, 12 and 16 % of the participant's body weight, and lasted for 150 ms. A recovery of the WBAM was seen directly after the perturbations, induced by adapting the moment arm of the GRF with respect to the CoM. The hip joint of the stance leg played an important role in achieving the WBAM recovery. A change in the direction of the GRF vector and not a contributing CoP modulation, caused the change in moment arm. However, the change in GRF direction came from a change in the horizontal GRF, which also affects the WBLM. This suggest that regulating WBAM may take precedence over the WBLM in early recovery.

1. Introduction

Healthy individuals highly regulate their whole body angular momentum (WBAM) during walking. This is achieved by segmental angular momentum cancellation and control of the ankle, knee and hip moments (Gruben and Boehm, 2014; Herr and Popovic, 2008; Neptune and McGowan, 2011; Pijnappels et al., 2004; Popovic et al., 2004; van Dieën et al., 2005). Tripping, slipping, or pushes applied above or below the body's centre of mass (CoM) can cause changes of the WBAM. An active response is required to prevent falling (Pijnappels et al., 2004, 2005). However, controlling joint moments to regulate the WBAM in case of a disturbance can be difficult for elderly or neuromuscular impaired people, for example due to a hemiparesis or spinal cord injury. A reduced ability for WBAM regulation increases the risk for falling in this group (Honda et al., 2019; Nott et al., 2014; Pijnappels et al., 2004, 2005; Simoneau and Krebs, 2000; van Dieën et al., 2005). Therefore, regulation of the WBAM is considered to be a crucial factor in balance recovery. A better understanding of human WBAM regulation is required for the use of WBAM regulation in a rehabilitation setting or in the development for controllers of assistive devices.

Previously, several experiments were performed with WBAM perturbations in standing and walking (van den Bogaart et al., 2020; Martelli et al., 2017; Pijnappels et al., 2004; Rietdyk et al., 1999; Schumacher et al., 2019). Often used perturbation methods are slipping or tripping by presenting obstacles, accelerating and decelerating the treadmill, or applying push or pull perturbations to the upper body (Martelli et al., 2017; Pijnappels et al., 2004; Rietdyk et al., 1999; Sessoms et al., 2014). However, these perturbation methods do not only influence the WBAM. Also the whole body linear momentum (WBLM) will be affected, which is proportional to the CoM velocity. This makes it more difficult to isolate strategies used in the regulation of the WBAM specifically. A study (by Schumacher et al. (2019)) managed to perturb the WBAM with minimal effect on the WBLM. They used an angular momentum perturbator (Lemus et al., 2017) worn as a backpack, containing a flywheel generating gyroscopic torques while participants were standing. Results from the above mentioned studies suggest a dominant role of regulating the hip joint moments in balance recovery from WBAM perturbations (Rietdyk et al., 1999; Schumacher et al., 2019). However, it is still unclear how recovery strategies are

* Corresponding author.
E-mail address: m.vanmierlo@utwente.nl (M. van Mierlo).

https://doi.org/10.1016/j.jbiomech.2022.111169
Accepted 26 May 2022
Available online 3 June 2022

Nomenclature

BPP	Backward pitch perturbation
CoM	Centre of mass
CoP	Centre of pressure
EndP	End perturbation
FPP	Forward pitch perturbation
GRF	Ground reaction force
HSL	Heel strike left
HSR	Heel strike right
QTM	Qualisys track manager
TOL	Toe off left
TOR	Toe off right
WBAM	Whole body angular momentum
WBLM	Whole body linear momentum

used during walking when mainly the WBAM in the sagittal plane is perturbed.

Changes in WBAM can be realized by creating joint moments to modulate the net moment of the ground reaction force (GRF) with respect to the CoM (Gruben and Boehm, 2014; Mathiyakom and McNitt-Gray, 2008). Modulation of this net moment is the result of a change in the moment arm of the GRF with respect to the CoM. The two options to influence this moment arm are discussed in the following paragraphs.

The first option to influence the moment arm is by changing the point of application of the GRF, visualized as centre of pressure (CoP) modulation in Fig. 1a. For example positioning the recovery limb more forward results in a forward shift of the CoP. This assists in recovery from a disturbance resulting in a forward rotation of the upper body (Mathiyakom and McNitt-Gray, 2008; Pijnappels et al., 2004). Another possibility to modulate the CoP position is by changing the ankle torque (Gruben and Boehm, 2014). A CoP modulation on its own could be used to create a moment arm affecting the WBAM without influencing the WBLM, since there is no change in horizontal GRF.

The second option to influence the moment arm about the CoM is by changing the direction of the GRF (Mathiyakom and McNitt-Gray, 2008). Directing the GRF anterior of the CoM results in a change of the WBAM rotating the upper body backward, visualized in Fig. 1b, and forward when the GRF passes posterior of the CoM. Pijnappels et al. (2005) showed that healthy individuals quickly recovered WBAM after tripping perturbations by generating joint moments in the supporting limb to redirect the GRF (Pijnappels et al., 2005). Especially the joint moments of the hip can play an important role in regulating the angular accelerations of the upper body (Klemetti et al., 2014). Changing the GRF direction can mainly be achieved by altering the horizontal component of the GRF. Although effective for restoring the WBAM, changing the horizontal GRF also affects WBLM. It is an open question whether this approach is also used after external perturbations that mainly perturb WBAM.

Being unable to regulate WBAM will increase the risk for falling, especially in case of a perturbation. Therefore, this study aims to increase understanding of how healthy individuals recover from WBAM perturbations in the sagittal plane, increasing insights into the fundamental human balance recovery strategies of the WBAM. This is done by applying two simultaneous perturbations in opposite directions to the pelvis and upper body. Since these perturbations theoretically do not affect the WBLM, we expect participants to use a recovery strategy that does not compromise the WBLM. Such a strategy would involve CoP modulation without change of the GRF direction, creating a moment arm about the CoM to recover WBAM. This could be achieved by modulating the ankle moment.

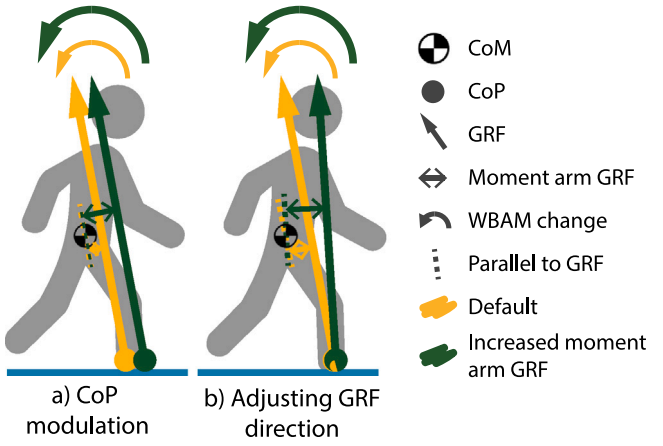

Fig. 1. Two methods of influencing the WBAM by changing the moment arm of the GRF with respect to the CoM. The green arrows show an example of how the moment arm can be increased with respect to the yellow case by (a) changing the position of the CoP and/or (b) adjusting the direction of the GRF. (For interpretation of the references to colour in this figure legend, the reader is referred to the web version of this article.)

2. Methods

2.1. Participants

Ten healthy volunteers (four men, age 24 ± 3 year, weight 66 ± 7 kg, height 1.75 ± 0.06 m, means ± SD) participated in the study. The local ethics committee approved the experimental setup and protocol. All participants gave written informed consent prior to the experiment in accordance with the Declaration of Helsinki.

2.2. Setup

Fig. 2 illustrates the setup. Participants walked on a split-belt instrumented treadmill (custom Y-Mill, Motek medical, Culemborg, The Netherlands). The 3D GRFs and moments were recorded with the force plates beneath each belt. Two motors (SMH60, Moog, Nieuw-Vennep, The Netherlands) were placed on the rear of the treadmill. Carbon lever arms with a length of 0.3 m were connected to the rotational axis of the motors. These lever arms were connected to horizontal carbon rods via ball joints. To control and measure the interaction forces with the participant, load cells (Model LRF350, FUTEK, Los Angeles, CA, USA) were integrated in the horizontal rods near the joints with the lever arms. On the other end, the rods were attached to the pelvis and upper body brace via ball joints. As pelvis brace a universal hip abduction brace (Distrac Wellcare, Hoegaarden, Belgium) and as upper body brace a body protector (USG Flexi body protector, Birstein, Germany) were used, to which connection joints for the rods were attached. The participants also wore a safety harness to prevent injury in case of a fall. The motors were placed on different heights such that the horizontal rod attached to the pelvis brace was at a height of 1.0 m from the treadmill surface and the one for the upper body at 1.4 m. The motors were controlled via the main computer (Linux, Ubuntu 16.04 LTS) and seven secundary devices: four Beckhoff modules (three analog input and one analog output, Beckhoff Automation GmbH, Germany), Haptic control unit (Moog PC CB79047-401_HCU, Nieuw-Vennep, The Netherlands) and two motor drives (Moog MSD 3200 Servo Drive, Nieuw-Vennep, The Netherlands). An admittance controller (described in van der Kooij et al. (2022)) was used to minimize the interaction forces during walking and to track the desired forces at the instant a perturbation was given.

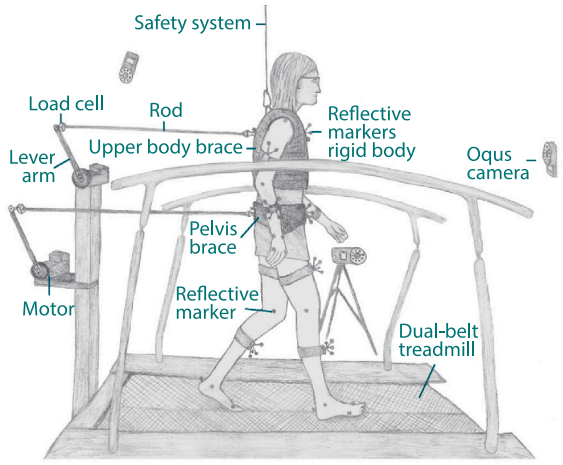

Fig. 2. Lab setup. A participant walking on the dual-belt treadmill with built-in force plates. Two motors are connected to the body via the lever arms, rods, and upper body brace and pelvis braces. This makes it possible to apply two simultaneous forces in opposite direction, resulting in moment around the CoM, but with a zero net force. The participant is connected to the ceiling via a safety system. Motion capture data is recorded with the Qualisys Oqus cameras.

2.3. Data collection

Kinematic data were recorded with an 8-camera passive Qualisys motion capture system (Oqus 600+, Qualisys, Göteborg, Sweden). Ten rigid bodies containing four reflective markers each were placed on the sternum, pelvis, upper and lower legs, upper arms, and forearms. Single markers were placed on the 7th cervical vertebra, and the left and right calcaneus, 1st and 5th metatarsal heads, medial and lateral malleoli, medial and lateral epicondyles of the femur, anterior and posterior superior iliac spines, acromia, medial and lateral humeral epicondyles, ulnar and radial styloids, and the 2nd and 5th metacarpal heads. The motion capture data was recorded at 128 Hz with the Qualisys Track Manager (QTM, Qualisys, Göteborg, Sweden). Via an analog interface (Kistler 5695A DAQ) data from the force plates was received at 2048 Hz in sync with the motion capture data. Data from the load cells integrated in the rods were recorded at 1000 Hz via the main computer controlling the motor, and synchronized with the other data via a synchronization signal.

2.4. Experimental protocol

The participants walked on the treadmill with a normal walking speed scaled to their leg length ($\sqrt{l} \cdot 1.25\,\mathrm{m\,s^{-1}}$). The experiment was divided into two blocks. The first block consisted of 3 min unperturbed walking to set a baseline. During the second block the participants received two simultaneous perturbations of the same magnitude in opposite direction on the pelvis and upper body. Backward perturbations on the pelvis and forward perturbations on the upper body will be called forward pitch perturbation (FPP), visualized in Fig. 3d. Forward perturbations on the pelvis and backward perturbations on the upper body are called backward pitch perturbation (BPP). All perturbations were given at the moment of toe off right (TOR), which was the instant the vertical GRF came below 5% of the participant's body weight. The individual perturbations lasted for 150 ms and had a magnitude of 4, 8, 12, and 16% of body weight. Each magnitude and direction was repeated 6 times, resulting in 48 perturbations, which were given in a randomized order. Between each perturbation there was a random interval ranging from 3 to 6 strides.

2.5. Data processing

QTM software was used to label the markers and interpolate the missing samples of the marker data with the polynomial gap filling tool. Processing of the data was done with Matlab (R2019b, MathWorks). The marker and force data were filtered with a 6th order zero phase low pass Butterworth filter with a cut off frequency based on the participant's cadence ($cadence \cdot 6.25\,\mathrm{Hz}$) (Rácz and Kiss, 2021). OpenSim 4.2 (Delp et al., 2007) was used to scale a full body model (Rajagopal et al., 2016), consisting of 22 segments, for each participant. The OpenSim inverse kinematics, inverse dynamics, and analyse tool were used to derive the joint moments and CoM positions, velocities and orientations of the total body and individual segments. The GRF and moment measurements were used to acquire the horizontal GRF component and to calculate the CoP position, which was expressed relative to the whole body CoM position. The moment arm of the GRF was calculated with respect to the CoM position obtained via OpenSim. The WBAM was calculated with Eq. (1), where i presents each body segment of the OpenSim model, x^i_{CoM} and x_{CoM} the position of each ith segment and the whole body CoM respectively, m_i each ith segment's mass, $\dot{x}^i_{CoM}$ and $\dot{x}_{CoM}$ the velocity of each ith segment and the whole body CoM respectively, I^i each ith segment's inertia tensor (obtained from the OpenSim model), and ω^i the angular velocity about the ith segment's CoM (Herr and Popovic, 2008). All measures are given in the global frame and in anteroposterior direction or about the mediolateral axis.

$$H = \sum_{i=1}^{22}[(x^i_{CoM} - x_{CoM}) \times m_i(\dot{x}^i_{CoM} - \dot{x}_{CoM}) + I^i\omega^i] \quad (1)$$

All measures were scaled for the individual participants by dividing through a scaling factor based on the participant's leg length (l), mass (m), height (h), and/or walking speed (ws) making the values dimensionless: $WBAM \rightarrow m \cdot h \cdot ws$; $velocity \rightarrow \sqrt{g \cdot l}$; $position \rightarrow l$. To bring the values back to the original order of magnitude, the scaled measures were multiplied with the measure-specific scaling factor calculated from the averages across all participants. All measures were also normalized over time by resampling each (gait) phase to 50 samples, synchronizing the instants of toe off, heel strike and the end of the perturbation (EndP). This allowed for averaging the data over all repetitions within each participant and across all participants.

2.6. Outcome measures

The outcome measures were defined as the maximal deviation of a measure due the perturbation with respect to the baseline value, which was recorded during unperturbed walking. This maximal deviation was taken at an instant during the left single support, between EndP and the instant the measure crossed the baseline value. It should be noted that these could have been taken at different instants of time for the different measures.

2.7. Statistics

Linear mixed models were used to evaluate the dependence of the outcome measures on the perturbations. The statistical analysis was performed in R4.1.2 (R Core Team, 2021, Vienna, Austria). Linear mixed models were fitted for each of the following outcome measures: WBAM, CoM velocity, moment arm of the GRF with respect to the CoM, CoP position with respect to the CoM, horizontal GRF and the joint moments of the hip, knee and ankle. Separate models were made for the FPP and BPP. The perturbation magnitude was added as a fixed effect. A shift of −4 or +4 was applied to the perturbation magnitude such that the intercept coincided with the smallest perturbation magnitude. Random effects for the intercept and slope were included to take into account the participant effects. The main effects were tested with a significance level of $\alpha = 0.05$ using the Wald t-test with a Kenward-Roger correction for the degrees of freedom.

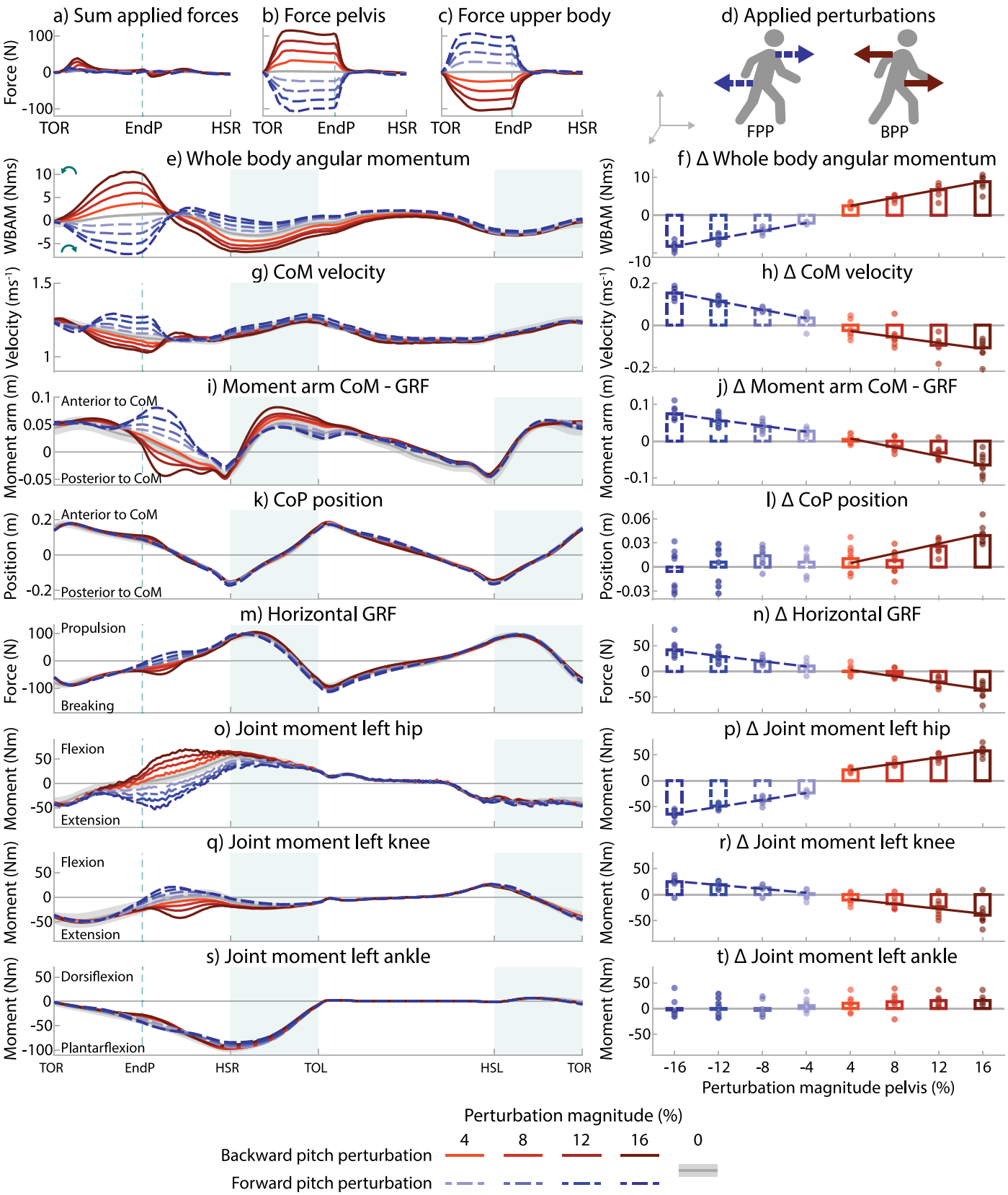

Fig. 3. The left column presents time series of one normalized gait cycle ranging from TOR to TOR. The perturbation starts at the first TOR and ends at EndP. Other marked events are heel strike right and left (HSR, HSL) and toe of left (TOL). Shaded areas indicate the double support phases. FPP are presented in blue and BPP in red. Unperturbed walking is presented in grey with an area covering the standard deviation. (a) shows the sum of the interaction forces measured in both rods. (b) Force pelvis and (c) Force upper body are the interaction forces of the motor connected to the pelvis and upper body brace respectively. The right column presents barplots of the outcome measures, maximum difference with respect to baseline between EndP and the instant the measure crossed the baseline value, for the different perturbation magnitudes. The dots present the averages per participant. Fitted models are included with a line if these were statistically significant ($p < 0.05$). The moment arm of the GRF is measured with respect to the CoM and the CoP position is presented with respect to the CoM. (For interpretation of the references to colour in this figure legend, the reader is referred to the web version of this article.)

Table 1
Estimated model parameters and model fits of the linear mixed models for the different outcome variables and perturbation directions (forward pitch and backward pitch). The intercept coincides with the smallest perturbation magnitude. All models had an N-value of 40 (4 magnitudes and 10 participants).

	Angular momentum (N m s)		**CoM velocity** ($m\,s^{-1}$)	
Fixed effect	Forward pitch	Backward pitch	Forward pitch	Backward pitch
Intercept	−2.033 ***	2.503 ***	0.033 ***	−0.028 *
Magnitude	0.507 ***	0.527 ***	−0.010 ***	−0.007 ***
Model fit				
R^2-marginal	0.91	0.79	0.82	0.39
R^2-conditional	0.99	0.98	0.92	0.86

	Moment arm (m)		**CoP position** (m)	
Fixed effect	Forward pitch	Backward pitch	Forward pitch	Backward pitch
Intercept	0.026 ***	0.007	0.012 *	0.005
Magnitude	−0.004 ***	−0.006 ***	0.001	0.003 ***
Model fit				
R^2-marginal	0.62	0.63	0.06	0.44
R^2-conditional	0.96	0.91	0.60	0.62

	Horizontal GRF (N)		**Joint moment hip** (N m)	
Fixed effect	Forward pitch	Backward pitch	Forward pitch	Backward pitch
Intercept	9.651 **	2.850	−23.909 ***	20.913 ***
Magnitude	−2.583 ***	−3.082 ***	3.354 ***	3.045 ***
Model fit				
R^2-marginal	0.53	0.63	0.86	0.83
R^2-conditional	0.93	0.92	0.94	0.97

	Joint moment knee (N m)		**Joint moment ankle** (N m)	
Fixed effect	Forward pitch	Backward pitch	Forward pitch	Backward pitch
Intercept	3.424	−8.800 *	2.655	10.854 *
Magnitude	−1.864 ***	−2.327 ***	0.555	0.450
Model fit				
R^2-marginal	0.48	0.31	0.03	0.03
R^2-conditional	0.87	0.83	0.73	0.85

The statistical significance of the parameters are indicated with the stars.
*$p < 0.05$.
**$p < 0.01$.
***$p < 0.001$.

3. Results

3.1. Perturbation effect

With a distance of 0.34 ± 0.03 m between the application points on the pelvis and upper body and a CoM position 0.01 ± 0.03 m above the pelvis point of application, the strongest perturbations (16%) resulted in a moment around the CoM of 35.2 N m on average. As intended, these perturbations induced a large, statistically significant (Table 1), change of the WBAM of about 2 N m s per perturbation level (Fig. 3e–f), with a positive change indicating a backward rotation of the upper body and vice versa. Beside the disturbance of the WBAM, unexpectedly the perturbations also affected the WBLM (Fig. 3g–h). A small CoM velocity change of $<0.04\,m\,s^{-1}$ per perturbation level was induced by the WBAM perturbations at EndP (Table 1). Assuming horizontal rods, simultaneous pelvis and upper body perturbations in opposite direction cause a cancellation of both motor forces. This resulted in a sum of the applied forces close to zero (Fig. 3a–c). An extended table containing all statistical test results can be found in the supplementary material.

3.2. Recovery of whole body angular momentum

After perturbations of the WBAM the moment arm of the GRF with respect to the CoM was adjusted (Fig. 3i–j). Directly after the FPP, an increase of the positive moment was observed. This implied that the GRF was passing more in front of the CoM, which contributed to counteracting the forward pitch due to the perturbation. This moment arm change was the result of a change in the horizontal GRF, which directed the GRF vector more forward. The horizontal GRF increased significantly with the increasing perturbation magnitude (Fig. 3m–n, Table 1). Meanwhile, no modulations were made to the CoP position with respect to the CoM (Fig. 3k–i).

The strong BPP (8, 12 and 16%) resulted in a GRF passing behind the CoM, helping recovery of the disturbed WBAM. Again, the change in horizontal GRF contributed to the creation of this moment arm, by directing the GRF backwards. On the other hand, the more forward positioned CoP due to the perturbation opposes the creation of this moment arm (Fig. 3l). However, this effect was not strong enough to overrule the change of the moment arm due to the horizontal GRF component.

3.3. Joint moment contributions

After perturbations of the WBAM, the hip of the stance leg generated a moment assisting in recovery of the WBAM (Fig. 3o–p). For the FPP this involved an extension moment and for the BPP a flexion moment. The knee contributed with an opposite response, applying a flexion moment after the FPP and an extension moment after the BPP (Fig. 3q–r). No modulations of the ankle moment were seen after perturbations of the WBAM (Fig. 3s–t).

4. Discussion

The goal of this study was to understand how healthy individuals recover balance when the WBAM is perturbed. By applying two simultaneous perturbations in opposite directions to the pelvis and upper body we were able to perturb the WBAM while keeping the effect on the WBLM limited. This allowed us to study the balance recovery when mainly the WBAM was perturbed. Contrary to what we hypothesized, the participants did not use a CoP modulation, but changed the direction of the GRF in order to recover the WBAM. Since this affects the horizontal GRF, which also affects the CoM velocity, we hypothesized the opposite. Possibly a trade off has been made in which the WBAM is prioritized over the WBLM. This notion is supported by earlier research showing that the CoM velocity increased due to the forward directed GRF used in the recovery of a trip rotating the upper body forward (Mathiyakom and McNitt-Gray, 2008).

Notable after the perturbations is the quick recovery response, especially compared to perturbations of the WBLM only (Vlutters et al., 2018a). Directly after EndP and before HSR the WBAM disturbance already reached a point of return, after which the WBAM gradually returned towards the baseline value over the following double and single support phases. For WBLM perturbations this point of return occurred later (Vlutters et al., 2018a). Since the WBAM perturbations mainly take place around the CoM, the hip strategy comprises a large part of the recovery. This strategy has to handle a moment of inertia with respect to the CoM. After the perturbations of the WBLM, an ankle strategy is used, involving a moment of inertia with respect to the ankle. The quicker response after WBAM perturbations compared to WBLM perturbations, might have been facilitated by the fact that the whole body moment of inertia with respect to the ankle is larger compared the whole body moment of inertia with respect to the CoM. Besides, according to Horak et al. (1997) humans create a "plan for action," weighting different control objectives based on desired targets. The head and trunk orientation are possibly highly-valued control objectives during normal walking (Horak et al., 1997). Also, it is

known that the human central nervous system highly regulates the WBAM, keeping deviations as small as possible (Herr and Popovic, 2008; Popovic et al., 2004). These findings and theories support the our observations of a quick recovery after perturbations of the WBAM.

Our results agree with previous findings of the importance of the hip strategy and a minor role of the ankle strategy in regulation of the WBAM (Best et al., 2019; Rietdyk et al., 1999; Schumacher et al., 2019). In contrast to perturbations of the WBLM only (Vlutters et al., 2018b), we did not see any involvement of the ankle joint after WBAM perturbations. This supports our findings that there was also no assisting CoP modulation, since changing the ankle moment would have influenced the CoP position (Gruben and Boehm, 2014). What we did see were strong hip flexion and extension moments that were generated such that these helped in bringing the upper body back to its initial orientation. These were accompanied by extension or flexion moments of the knee joint respectively. Simultaneous hip flexion and knee extension or hip extension and knee flexion suggests involvement of bi-articular muscles, the rectus femoris and biceps femoris respectively. This agrees with the results of Schumacher et al. (2019), who reported strong involvements of the biarticular thigh muscles in counteracting upper-body pitch perturbations during standing. Overall our results confirm the important role of the hip in recovering from WBAM perturbations.

Changing the moment arm of the GRF with respect to the CoM to recover from the perturbations, was done by altering the GRF direction, without contributing CoP modulation. Even though theoretically a CoP modulation would be effective in counteracting WBAM perturbations, previous studies also did not see modulations of the mediolateral CoP position through modulations of the foot placement and/or ankle moment after upper body perturbations in the frontal plane during standing (Rietdyk et al., 1999) and walking (Best et al., 2019). In contrast, after perturbations of only the WBLM during walking, various studies did report modulations of the CoP, foot placement, and/or horizontal GRF in the frontal and sagittal plane after perturbations of only the WBLM during walking (Bruijn and Dieën, 2018; Hof et al., 2010; Vlutters et al., 2016; Wang and Srinivasan, 2014; Zadravec et al., 2017).

A limitation of our study is the use of an OpenSim model without a neck joint. Since a marker configuration without head markers was used, an over-estimation of the head excursion may occur in the OpenSim model, as it is rigidly linked to the upper body. This possibly caused the more extreme values of the WBAM, and also the unexpected change of the CoM velocity during the WBAM perturbation, while the net horizontal force did not change during that phase. This makes it likely that the reported CoM velocity deviations during the perturbation can be considered as an artifact. For future studies perturbing the upper body it is recommended to use a model including the neck joint and to apply more markers on the torso and head to gain a better measurement of the upper body motion.

The ability of estimating how to continue walking without falling can be valuable for the development of balance controllers for assistive devices like lower limb exoskeletons. However, only using the CoM velocity for this estimation might not be sufficient in case of a perturbation above or below the CoM resulting in changes of the WBAM. After these perturbations other recovery strategies are required that take into account the WBAM, for example by using a momentum-based control algorithm (Bayon et al., 2020). Besides that, we should also keep in mind that humans prioritize in the recovery strategies (Horak et al., 1997). It seems that recovering the WBAM has priority, which is even done at the expenses of the CoM velocity regulation. To extend these results it would also be interesting to study responses to WBAM perturbations in the frontal plane or during different conditions like walking speed.

To conclude, healthy individuals quickly recover from WBAM perturbations given at toe off by using the hip of the stance leg to create a GRF passing in front of- or behind the CoM, resulting in a change of the WBAM. This is done without CoP modulations contributing to the WBAM recovery. This WBAM recovery strategy might affect the WBLM, suggesting that recovering the WBAM was prioritized over the WBLM.

CRediT authorship contribution statement

M. van Mierlo: Writing – original draft, Visualization, Software, Methodology, Investigation, Formal analysis, Conceptualization. **J.I. Ambrosius:** Writing – review & editing, Investigation. **M. Vlutters:** Writing – review & editing, Software, Methodology, Conceptualization. **E.H.F. van Asseldonk:** Writing – review & editing, Supervision, Methodology, Conceptualization. **H. van der Kooij:** Writing – review & editing, Supervision, Project administration, Methodology, Funding acquisition, Conceptualization.

Declaration of competing interest

The authors declare that they have no known competing financial interests or personal relationships that could have appeared to influence the work reported in this paper.

Data availability

The data used for this study is published on 4TU.ResearchData and can be found via the following DOI: http://dx.doi.org/10.4121/19307225.

Acknowledgements

This work is part of the research program Wearable Robotics with project number P16-05, which is (partly) funded by the Dutch Research Council (NWO), The Netherlands.

Appendix A. Supplementary data

Supplementary material related to this article can be found online at https://doi.org/10.1016/j.jbiomech.2022.111169.

References

Bayon, C., Emmens, A.R., Afschrift, M., van Wouwe, T., Keemink, A.Q.L., van der Kooij, H., van Asseldonk, E.H.F., 2020. Can momentum-based control predict human balance recovery strategies? IEEE Trans. Neural Syst. Rehabil. Eng. 28 (9), 2015–2024. http://dx.doi.org/10.1109/TNSRE.2020.3005455.

Best, A.N., Martin, J.P., Li, Q., Wu, A.R., 2019. Stepping behaviour contributes little to balance control against continuous mediolateral trunk perturbations. J. Exp. Biol. 222 (24), http://dx.doi.org/10.1242/jeb.212787.

van den Bogaart, M., Bruijn, S.M., van Dieën, J.H., Meyns, P., 2020. The effect of anteroposterior perturbations on the control of the center of mass during treadmill walking. J. Biomech. 103, 109660. http://dx.doi.org/10.1016/j.jbiomech.2020.109660.

Bruijn, S.M., Dieën, J.H.V., 2018. Control of human gait stability through foot placement. J. R. Soc. Interface 15 (20170816), http://dx.doi.org/10.1098/rsif.2017.0816.

Delp, S.L., Anderson, F.C., Arnold, A.S., Loan, P., Habib, A., John, C.T., Guendelman, E., Thelen, D.G., 2007. OpenSim: OPen-source software to create and analyze dynamic simulations of movement. IEEE Trans. Biomed. Eng. 54 (11), 1940–1950. http://dx.doi.org/10.1109/TBME.2007.901024.

Gruben, K.G., Boehm, W.L., 2014. Ankle torque control that shifts the center of pressure from heel to toe contributes non-zero sagittal plane angular momentum during human walking. J. Biomech. 47 (6), 1389–1394. http://dx.doi.org/10.1016/j.jbiomech.2014.01.034.

Herr, H., Popovic, M., 2008. Angular momentum in human walking. J. Exp. Biol. 211 (4), 467–481. http://dx.doi.org/10.1242/jeb.008573.

Hof, A.L., Vermerris, S.M., Gjaltema, W.A., 2010. Balance responses to lateral perturbations in human treadmill walking. J. Exp. Biol. 213, 2655–2664. http://dx.doi.org/10.1242/jeb.042572.

Honda, K., Sekiguchi, Y., Muraki, T., Izumi, S.I., 2019. The differences in sagittal plane whole-body angular momentum during gait between patients with hemiparesis and healthy people. J. Biomech. 86, 204–209. http://dx.doi.org/10.1016/j.jbiomech.2019.02.012.

Horak, F.B., Henry, S.M., Shumway-Cook, A., 1997. Postural perturbations: New insights for treatment of balance disorders. Phys. Ther. 77 (5), 517–533. http://dx.doi.org/10.1093/ptj/77.5.517.

Klemetti, R., Steele, K.M., Moilanen, P., Avela, J., Timonen, J., 2014. Contributions of individual muscles to the sagittal- and frontal-plane angular accelerations of the trunk in walking. J. Biomech. 47 (10), 2263–2268. http://dx.doi.org/10.1016/j.jbiomech.2014.04.052.

van der Kooij, H., Fricke, S.S., van 't Veld, R.C., Prieto, A.V., Keemink, A.Q.L., Schouten, A.C., van Asseldonk, E.H.F., 2022. Identification of hip and knee joint impedance during the swing phase of walking. IEEE Trans. Neural Syst. Rehabil. Eng. 28, 2015–2024. http://dx.doi.org/10.1109/TNSRE.2022.3172497.

Lemus, D., van Frankenhuyzen, J., Vallery, H., 2017. Design and evaluation of a balance assistance control moment gyroscope. J. Mech. Robot. 9, 1–9. http://dx.doi.org/10.1115/1.4037255.

Martelli, D., Aprigliano, F., Tropea, P., Pasquini, G., Micera, S., Monaco, V., 2017. Stability against backward balance loss: Age-related modifications following slip-like perturbations of multiple amplitudes. Gait Posture 53, 207–214. http://dx.doi.org/10.1016/j.gaitpost.2017.02.002.

Mathiyakom, W., McNitt-Gray, J.L., 2008. Regulation of angular impulse during fall recovery. J. Rehabil. Res. Dev. 45 (8), 1237–1248. http://dx.doi.org/10.1682/JRRD.2008.02.0033.

Neptune, R., McGowan, C., 2011. Muscle contributions to whole-body sagittal plane angular momentum during walking. J. Biomech. 44 (1), 6–12. http://dx.doi.org/10.1016/j.jbiomech.2010.08.015.

Nott, C.R., Neptune, R.R., Kautz, S.A., 2014. Relationships between frontal-plane angular momentum and clinical balance measures during post-stroke hemiparetic walking. Gait Posture 39 (1), 129–134. http://dx.doi.org/10.1016/j.gaitpost.2013.06.008.

Pijnappels, M., Bobbert, M.F., van Dieën, J.H., 2004. Contribution of the support limb in control of angular momentum after tripping. J. Biomech. 37 (12), 1811–1818. http://dx.doi.org/10.1016/j.jbiomech.2004.02.038.

Pijnappels, M., Bobbert, M.F., van Dieën, J.H., 2005. How early reactions in the support limb contribute to balance recovery after tripping. J. Biomech. 38 (3), 627–634. http://dx.doi.org/10.1016/j.jbiomech.2004.03.029.

Popovic, M., Hofmann, A., Herr, H., 2004. Angular momentum regulation during human walking: Biomechanics and control. Proc. IEEE Int. Conf. Robot. Autom. 2405–2411.

R Core Team, 2021. R: A Language and Environment for Statistical Computing. R Foundation for Statistical Computing, Vienna, Austria, URL: https://www.R-project.org/.

Rácz, K., Kiss, R.M., 2021. Marker displacement data filtering in gait analysis: A technical note. Biomed. Signal Process. Control 70, 102974. http://dx.doi.org/10.1016/j.bspc.2021.102974.

Rajagopal, A., Dembia, C.L., Demers, M.S., Delp, D.D., Hicks, J.L., Delp, S.L., 2016. Full body musculoskeletal model for muscle-driven simulation of human gait. IEEE Trans. Biomed. Eng. 63 (10), 2068–2079. http://dx.doi.org/10.1109/TBME.2016.2586891.

Rietdyk, S., Patla, A.E., Winter, D.A., Ishac, M.G., Little, C.E., 1999. Balance recovery from medio-lateral perturbations of the upper body during standing. J. Biomech. 32, 1149–1158.

Schumacher, C., Berry, A., Lemus, D., Rode, C., Seyfarth, A., Vallery, H., 2019. Biarticular muscles are most responsive to upper-body pitch perturbations in human standing. Sci. Rep. 9 (1), http://dx.doi.org/10.1038/s41598-019-50995-3.

Sessoms, P.H., Wyatt, M., Grabiner, M., Collins, J.D., Kingsbury, T., Thesing, N., Kaufman, K., 2014. Method for evoking a trip-like response using a treadmill-based perturbation during locomotion. J. Biomech. 47 (1), 277–280. http://dx.doi.org/10.1016/j.jbiomech.2013.10.035.

Simoneau, G.G., Krebs, D.E., 2000. Whole-body momentum during gait: A preliminary study of non-fallers and frequent fallers. J. Appl. Biomech. 16 (1), 1–13. http://dx.doi.org/10.1123/jab.16.1.1.

van Dieën, J.H., Pijnappels, M., Bobbert, M.F., 2005. Age-related intrinsic limitations in preventing a trip and regaining balance after a trip. Saf. Sci. 43 (7), 437–453. http://dx.doi.org/10.1016/j.ssci.2005.08.008.

Vlutters, M., van Asseldonk, E.H.F., van der Kooij, H., 2016. Center of mass velocity-based predictions in balance recovery following pelvis perturbations during human walking. J. Exp. Biol. 219 (10), 1514–1523. http://dx.doi.org/10.1242/jeb.129338.

Vlutters, M., van Asseldonk, E.H.F., van der Kooij, H., 2018a. Foot placement modulation diminishes for perturbations near foot contact. Front. Bioeng. Biotechnol. 6 (48), 1–14. http://dx.doi.org/10.3389/fbioe.2018.00048.

Vlutters, M., van Asseldonk, E.H.F., van der Kooij, H., 2018b. Lower extremity joint-level responses to pelvis perturbation during human walking. Sci. Rep. 8 (1), 14621. http://dx.doi.org/10.1038/s41598-018-32839-8.

Wang, Y., Srinivasan, M., 2014. Stepping in the direction of the fall : the next foot placement can be predicted from current upper body state in steady-state walking. Biol. Lett. 10 (20140405), http://dx.doi.org/10.1098/rsbl.2014.0405.

Zadravec, M., Olenšek, A., Matjačić, Z., 2017. The comparison of stepping responses following perturbations applied to pelvis during overground and treadmill walking. Technol. Health Care 25, 781–790. http://dx.doi.org/10.1007/978-3-319-46669-9_50.